MANSOURA JOURNAL OF CHEMISTRY
Official Journal of Faculty of Science, Mansoura University, Egypt
E-mail: scimag@mans.edu.eg ISSN: 2974-4938

Corrosion inhibition of carbon steel by utilizing 1-(α-naphthoxyacetyl)-4-ethyl-3-thiosemicarbazide in 1M HCl solution

Kamelia Belal, A.H. El-Askalany, O.A. El-Gammal,and Ahmed Fathi Salem Molouk*

Department of Chemistry, Faculty of Science, Mansoura University, Mansoura 35516, Egypt

Email: *molouk82@mans.edu.eg*...***Tel: 01025394780***

Received:3/10/2023
Accepted:15/11/2023

Abstract: The current study examines the use of 1-(naphthoxyacetyl)-4-ethyl-3-thiosemicarbazide (H2NAET) as an inhibitor against corrosion in 1 M HCl. Mass loss (ML) and potentiodynamic polarization (PP) studies are two methods used to confirm the tested compound's inhibitory effect. The results show that increasing the temperature and inhibitor concentration improved inhibition potency. The adsorption of H2NAET on carbon steel follows the Langmuir adsorption isotherm and the inhibitor functions as mixed corrosion inhibitor. Atomic force microscopy (AFM) was used to analyze the surface. The gathered data showed that a preservative layer of the inhibitor had developed on the surface of the carbon steel.

keywords: CS, **H2NAET**, HCl

1.Introduction

Carbon steel (CS) is one of the materials that is most used for pipelines, ship equipment, tanks, and petroleum applications, it has exceptional qualities like ease of manufacture, low cost, and the capacity to maintain its characteristics at high temperatures. However, when exposed to acidic solutions, CS is susceptible to corrosion [1]. There are various ways to handle this issue, but using corrosion inhibitors has emerged as the most effective method for increasing the resistance of metals and reducing corrosion. The corrosion rate is significantly reduced when such compounds are added to acidic solutions [2].

Organic molecules having heteroatoms (N, S, O, etc.), π-electrons, and aromatic rings were used to avoid metal corrosion in various corrosive conditions [3]. The mechanism of inhibition may be physical adsorption, which results from electrostatic interactions among charged molecules and the metal surface, or chemisorption, which is accomplished by electron sharing between inhibitors and the metal's d-orbital [4]. Thiosemicarbazide derivatives have a unique affinity for reducing the corrosive action of acids on metals [5-10]. The novelty of this study is to prepare a novel corrosion inhibitor, namely 1-(α-naphthoxyacetyl)-4-ethyl-3-thiosemicarbazide (H2NAET), which was not discussed before as protecting material for CS corrosion in 1.0 M HCl. Moreover, this work targeted the use of low-concentration content of the tested inhibitor to be more cost-effective. Therefore, the performance of **H2NAET** was tested towards carbon steel corrosion in 1.0 M HCl utilizing ML and PP approaches.

2. Materials and methods

2.1Metallic Materials

The CS samples were composed of C 0.2%, S 0.05%, Mn 0.5%, Si 0.25%, and Fe 99%. For the ML test, the sheet has been chopped into samples with dimensions 2.2 × 1.6 × 0.2 cm (L x W x H), whereas the working electrode for the PP method has a surface area of 0.8 cm^2. Before any test, the CS surface was mechanically polished by different grades of emery papers (400, 1000, 1200, 2000), rinsed utilizing bi-distilled water, and then dried via filter papers.

2.2 Solutions

To prepare 1 M HCl, the analytical reagent grade 37% HCl (Acros Organics Brand, supplied by Cornell Lab, Egypt) was diluted with bi-distilled water. By diluting the stock solution (10^{-3} M) with bi-distilled water, the

appropriate concentrations of **H2NAET** (1–9 x 10^{-5} M) were obtained.

2.3 Synthesis of the inhibitor

α -Naphthoxyacetylhydrazine was synthesized according to the literature method [11]. **H2NAET** was synthesized by mixing ethyl isothiocyanate and α-naphthoxyacetylhydrazine in 100 ml absolute ethanol under reflux for 1 h. Upon cooling, white precipitate was collected, filtered out, washed, and recrystallized from absolute ethanol before being dehydrated in desiccator above anhydrous calcium chloride. The white precipitate powder is 1-(α-naphthoxyacetyl)-4-ethyl-3-thiosemicarbazide (H2NAET) in ≈ 24.7 gm yield, m.p. 180˚C as mentioned in the literature [12]. $C_{15}H_{17}$ N_3O_2S (303.38); Elemental Anal. % Found (Calcd): C 59.65 (59.39), H 5.44 (5.65), N 13.55 (13.85). FTIR (cm^{-1}): 1695 ν (C=O), 890 ν (C=S), 1224 ν (CS) + ν (CN), 1010 ν (N-N). No bands found above 3500 cm^{-1} or in the 2500-2600 cm^{-1} region which could be due to ν(OH) and ν(SH) vibrations, respectively. The absence of these bands reveals the existence of the thiosemicarbazide in thione/keto form. ^{1}H NMR spectrum: three signals at δ 10.11, 9.28 and 8.46 ppm, ascribed to N (1) H, N (2) H and N (4)H protons, respectively which disappear upon adding D_2O. The multiple signals at δ 3.35-3.51 ppm may be owing to the protons of -CH_2 and -CH_3 groups. Also, the multiplets at δ7.41-8.61 ppm are owing to the protons of naphthyl ring.

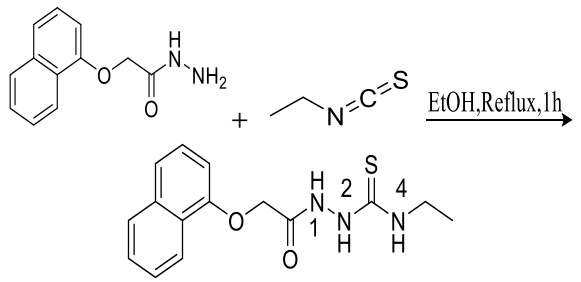

2.4 Mass loss method

The CS sheets were pretreated, dried, and then weighed. The specimens were subsequently immersed in HCl solution using a glass hook for six hours at various temperatures (25–45 °C), without and with the addition of different concentrations of **H2NAET**. The specimens were taken out every hour, cleaned, dried, and weighed once more. The inhibition efficiency (%IE) and the surface coverage (θ) of **H2NAET** were computed using Eq. (1) [13].

%IE= θ x100=[1-(W/W^o)]x100, (1) where (W^o) and (W) represent the average weight loss without and with the existence of the inhibitor, respectively.

2.5 PP method

A working electrode, a reference electrode, and an auxiliary electrode were utilized in this approach, which was conducted in a glass cell. The working electrode was the CS. The platinum sheet was employed as the counter electrode and an electrode made of silver/silver chloride (Ag/AgCl) as the reference electrode. At 25°C, the electrodes were submerged in 1 M HCl then with adding various concentrations of **H2NAET**. Using a scan rate of 5 mV/s, a potential of ± 500 mV was applied for the Tafel polarization test. The corrosion current (icorr) value was calculated by extrapolating of cathodic and anodic (βc & βa) tafel slopes of the curves. Eq. (2) was employed to get %IE as well as θ [14].

%IE= θ x100=[1-(i_{corr}/i^o_{corr})]x100, (2) where. (i^o_{corr}) and (i_{corr}) represent the corrosion current densities without and with utilizing the inhibitor, respectively.

This test was accomplished utilizing Potentiostat/Galvanostat/Zra analyzer (Gamry 5000E, USA).

2.6 Surface Examinations

The morphology of CS surface was examined after dipping into 1 M HCl without and with the addition of 9x10^{-5} M of **H2NAET** at 25°C for 24 h via AFM analysis (Nanosurf FlexAFM 3, Gräubernstrasse 12, 4410 Liestal, Switzerland) at Faculty of Engineering, Mansoura University.

3. Results and Discussion

3.1 ML method

At different time durations, the mass loss of CS was investigated without and with utilizing various concentrations **H2NAET**. Fig. 1 displays the obtained ML-time curves for **H2NAET**. There is a linear relationship between time and the weight loss of CS in the existence of **H2NAET**. Additionally, the weight loss was markedly reduced with the addition of **H2NAET** as compared to the blank

solution (1M HCl). This indicates that **H2NAET** was initially adsorbed on the CS surface then reduces the dissolution process [15]. The value of % IE was dependent on the inhibitor concentration. Table 1 lists the corrosion parameters for **H2NAET** at 25℃.

3.2 Effect of Temperature

To study how the temperature affects the effectiveness of **H2NAET** in 1 M HCl, ML measurements were monitored utilizing various concentrations at temperatures ranging from 25 to 45 ℃. According to Table 2, as the temperature rises, CR and the %IE of **H2NAET** both rises. The adsorption behavior of **H2NAET** on CS may therefore be the result of chemical adsorption [16].

3.3 Adsorption Isotherms

The type of adsorption isotherm could be used to investigate how **H2NAET** adsorbed onto CS. To determine which isotherm model best matches the experimental results, various isotherm models including Freundlich, Frumkin, Temkin, and Langmuir were examined. Based on the data gathered, the adsorption follows the Langmuir adsorption isotherm. Each adsorption site on a metal surface has a specific number of adsorbed species, according to the Langmuir model. Plotting of C/θ versus C for **H2NAET** gives straight lines (Fig.2) with correlation coefficient (R^2) close to unity, slope nearly equals unity, and intercept equal $1/K_{ads}$ according to Eq. (3)[17].

$C/\theta=1/K_{ads}+C$, (3) where C denotes the inhibitor concentration (M), θ represents the degree of surface coverage as well as K_{ads} is the equilibrium constant (M^{-1}) which is linked to the standard free energy of adsorption (ΔG^o_{ads}) according to Eq. (4) [18].

$\Delta G^o_{ads}= -2.303RT\log (K_{ads}x55.5)$, (4)

where the constant 55.5 is the water concentration (mole/L), R denotes the universal gas constant (8.314 J K^{-1} mol^{-1}), and T is the absolute temperature in kelvin. To determine the standard heat of adsorption ($\Delta H°_{ads}$), the Van't Hoff Eq. (5) was applied via plotting log K_{ads} versus 1/T as illustrated in Fig. 3, and the thermodynamic basic Eq. (6) was utilized to get the standard entropy of adsorption ($\Delta S°_{ads}$) [16].

$\log K_{ads}=(-\Delta H°_{ads})/2.303RT+constant$, (5)

$\Delta G^o_{ads}=\Delta H°_{ads}-T\Delta S°_{ads}$, (6) The estimated parameters were mentioned in Table 3 with the negative values of $\Delta G°_{ads}$ indicating the spontaneity of the adsorption process. Generally, if the ΔG^o_{ads} values close to - 40 kJ mol^{-1} or higher negative, the adsorption takes place through chemical interaction (chemisorption), which includes sharing or transfer of charge from the inhibitor to the metal surface to establish a coordinate bond, and through electrostatic interaction (physisorption) if they are close to -20 kJ mol^{-1} or less negative. The measured values of $\Delta G°_{ads}$ are in the range of -40 kJ mol^{-1}, confirming the hypothesis that chemisorption is probably dominant[19]. ΔH^o_{ads} values that are negative correspond to exothermic adsorption processes, while positive values correspond to endothermic processes. From the literature, it is well established that inhibitor molecules undergo chemisorption when the adsorption process is endothermic (positive ΔH^o_{ads}), whereas physisorption is indicated by an exothermic (negative ΔH^o_{ads}) process. It is confirmed that **H2NAET** is chemically adsorbed on the CS surface in the current work by ΔH^o_{ads} positive values, which indicate that the adsorption process is endothermic[20]. Due to the adsorption of **H2NAET** on the CS, the values of ΔS^o_{ads} show that the process coincides with an increase in disorder[21].

3.4 PP Measurements

Fig. 4 shows the PP curve of CS using 1M HCl before as well as after adding different concentrations of **H2NAET** at 25 °C. Table 4 displays the PP parameters including the corrosion current density (i_{corr}), corrosion potential (E_{corr}), and tafel slopes (β_a, β_c). According to PP curves, compared to the blank solution, the existence of **H2NAET** reduces the current density of the anodic and cathodic branches. Additionally, it was discovered that i_{corr} decreases and %IE increases as the concentration of **H2NAET** rises [22]. At 25°C, tafel slopes do not significantly alter with the addition of **H2NAET**, implying that its existence does not affect on the mechanism of corrosion process as well as hydrogen evolution. The slight change in E_{corr} indicates that **H2NAET** behaved as a mixed inhibitor that affected both the anodic and cathodic

processes [23]. Furthermore, the polarization resistances (Rp) for CS/HCl system with different concentrations of **H2NAET** were calculated according to the following equation:

$$Rp=\frac{\beta_a\beta_c}{2.303(\beta_a+\beta_c)i_{corr}} \quad (7)$$

where, i_{corr} is the corrosion current density. β_a and β_c are the anodic and cathodic Tafel slope, respectively. The Rp increased significantly with increasing **H2NAET** concentration, confirming the formation of the adsorbed layer from **H2NAET** on the CS surface which increased with increasing concentration, as it can be seen from the surface coverage (θ), hindering the rate of corrosion process for CS.

3.5 Surface Examination

3.5.1 AFM technique

AFM is a technique that is carried out to examine the surface morphology, roughness, and efficiency of **H2NAET** toward the corrosion of CS. Three-dimensional AFM images are displayed in Fig. 5 for polished CS surface, immersed CS surface in 1 M HCl as well as with the existence of an optimum concentration of H2NAET for 24 hours. In 1M HCl, the surface of the CS was seen to be rough, whereas in the existence of **H2NAET**, the surface is less corroded and seems to be considerably smoother. The average roughness measurements were made for the polished surface of CS (Fig. 5a) and the surfaces of CS in 1 M HCl (Fig. 5b), and the results were 6.91 nm and 652.06 nm, respectively. In the existence of **H2NAET**, the surface gets smoother, and the average roughness is minimized to 263.28 nm, respectively, as shown in Fig. 5c. This demonstrates the adsorption of **H2NAET** on the CS surface[24]. These roughness values support the data obtained by utilizing the ML and PP methods.

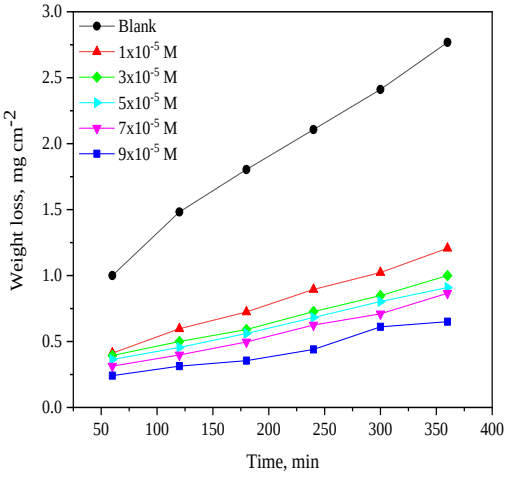

Figure 1: ML-time plot for the dissolution of CS in 1M HCl without and with adding different concentrations of **H2NAET** at 25°C

Table 1 ML parameters calculated after 300 minutes of immersing CS in 1 M HCl before and after adding various

concentrations of **H2NAET** at 25 °C.

Inhibitor	Conc. x10^{-5} (M)	CR (mg.cm^{-2}.min^{-1})	θ	% IE
1M HCl	Blank	0.0080	--	--
H2NAET	1	0.0034	0.575	57.5
	3	0.0028	0.650	65.0
	5	0.0027	0.663	66.3
	7	0.0024	0.700	70.0
	9	0.0020	0.750	75.0

Table 2 ML parameters calculated after 300 minutes of immersing CS in 1 M HCl before and after adding various

concentrations of **H2NAET** at 25 -45 °C.

Inhibitor	Conc.(M)	25°C		30°C		35°C		40°C		45°C	
		CR	%IE	CR	% IE	CR	%IE	CR	%IE	CR	%IE
Blank	1M HCl	0.0080	--	0.0115	--	0.0170	--	0.0277	--	0.0430	--
H2NAET	1 x10^{-5}	0.0034	57.5	0.0041	64.3	0.0059	65.3	0.0085	69.3	0.0128	70.2
	3 x10^{-5}	0.0028	65.0	0.0036	68.7	0.0052	69.4	0.0072	74.0	0.0104	75.8
	5 x10^{-5}	0.0027	66.3	0.0032	72.2	0.0044	74.1	0.0062	77.6	0.0082	80.9
	7 x10^{-5}	0.0024	70.0	0.0025	78.3	0.0036	78.8	0.0051	81.6	0.0073	83.0
	9 x10^{-5}	0.0020	75.0	0.0022	80.9	0.0031	81.8	0.0040	85.6	0.0056	87.0

Table 3 Adsorption isotherm parameters for **H2NAET** in 1 M HCl at various temperatures.

Inhibitor	Temp (°C)	K_{ads} x 10^4(M^{-1})	$-\Delta G°_{ads}$ (KJ mol^{-1})	$\Delta H°_{ads}$ (KJ mol^{-1})	$\Delta S°_{ads}$ (J mol^{-1} K^{-1})
H2NAET	25	14.5	39.40	15.01	182.58
	30	14.8	40.11		181.91
	35	16.1	40.99		181.82
	40	18.8	42.05		182.30
	45	20.8	43.00		182.42

Table 4 The PP parameters of **H2NAET** for CS in 1 M HCl at 25°C.

Inhibitor	Conc. (M)	$i_{corr.}$ µA.cm^{-2}	$-E_{corr.}$ mVvs.Ag/AgCl	β_a $mVdec^{-1}$	β_c $mVdec^{-1}$	Rp Ωcm^2	CR Mpy	θ	%IE
Blank	**1M HCl**	**226.3**	**463**	**42.30**	**109.9**	**58.60**	**82.68**	---	---
H2NAET	1x10^{-5}	88.3	455	117.5	154.3	328.0	40.29	0.610	61.0
	3 x10^{-5}	79.5	457	128.5	167.5	397.2	36.31	0.649	64.9
	5 x10^{-5}	63.9	460	125.5	162.4	481.1	29.18	0.718	71.8
	7 x10^{-5}	53.6	450	119.4	160.1	554.1	24.48	0.763	76.3
	9 x10^{-5}	44.0	458	143.0	173.8	774.2	20.10	0.806	80.6

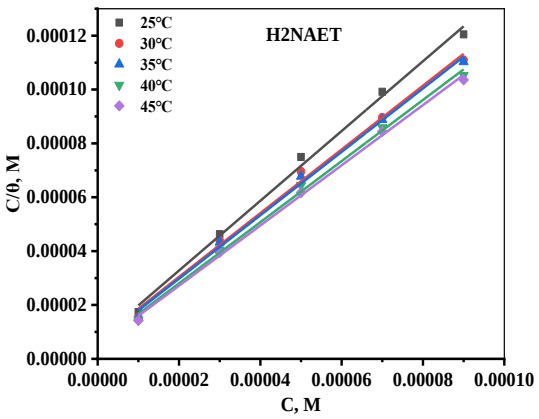

Figure 2: Langmuir adsorption isotherm of **H2NAET** in 1 M HCl at various temperatures.

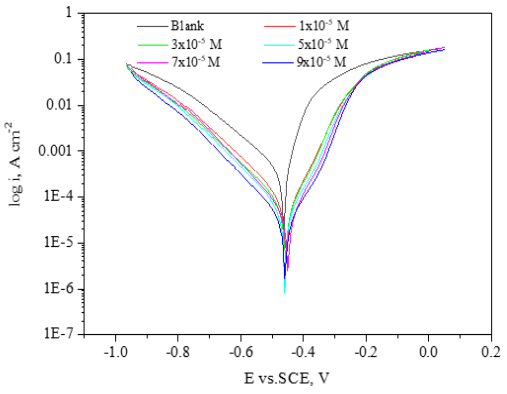

Figure 4: PP curve for CS utilizing a solution of 1 M HCl without and with the addition of various concentrations of **H2NAET** at 25°C.

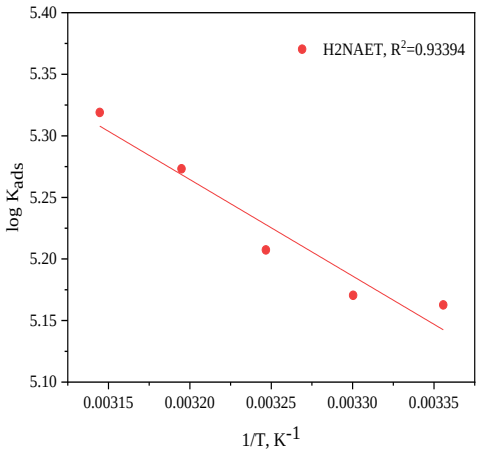

Figure 3: log K_{ads} versus (1/T) for CS utilizing 1 M HCl in the existence of **H2NAET**.

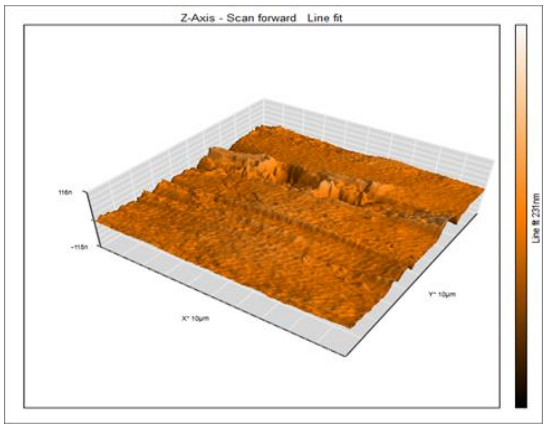

(a) Polished surface

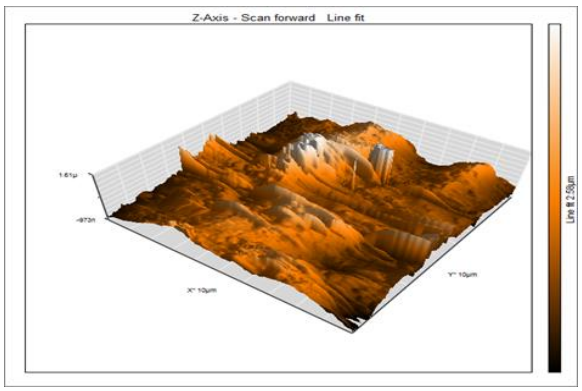

(b)Blank

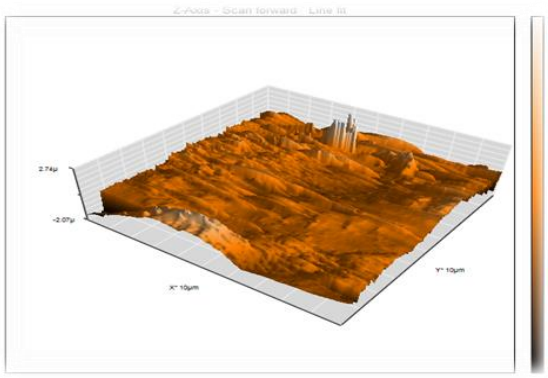

(c)H2NAET

Figure 5: AFM images for CS: Polished CS (a); CS immersed in HCl solution (b); CS immersed in HCl solution including **H2NAET** (c)

Possible mechanism of corrosion inhibition

The initial stage of any corrosion inhibition is the inhibitor's adsorption on the CS surface. The gathered data indicates that **H2NAET** is adsorbed on the CS surface by a chemical reaction in which unpaired electrons from inhibitor molecules (H2NAET) are transferred to the vacant d orbital of iron atoms at the CS surface. This process results in the formation of coordination bonds and a very stable complex from the inhibitor molecules that covers the CS surface as a protective layer. Because of the location of the naphthalene and the functional groups thione, carbonyl, and amino, the inhibitor is a charged molecule with a strong inductive and extremely strong resonance effect. The inclusion of thione and carbonyl groups and the aromatic ring increases electron delocalization, making it more reactive. Although carbonyl, thione, and amine (oxygen, sulfur, and nitrogen atoms) all have a single pair of electrons, the inhibitor is preferentially adsorbed onto the metal surface through these functional groups. Fig. 6, illustrates the proposed mechanism of inhibition via chemisorption.

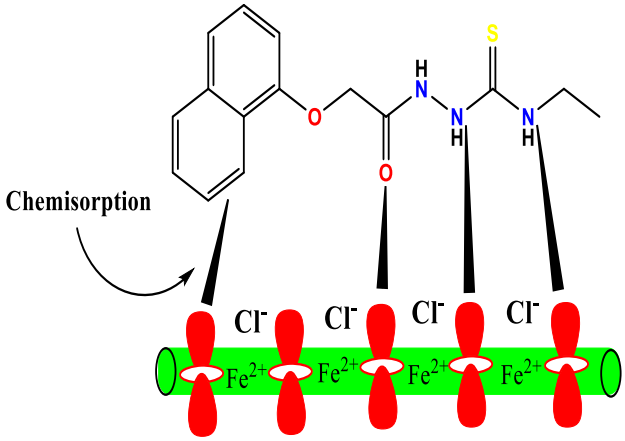

Figure 6: The suggested inhibition mechanism of **H2NAET** on CS surface.

4. Conclusions

H2NAET provides a good protection for CS in 1M HCl solution via adsorption on its surface. The potency of **H2NAET** to prohibit dissolution rises with concentration and temperature. The adsorption of **H2NAET** follows Langmuir adsorption isotherm with the assumption that mixed adsorption (physisorption and chemisorption) occurs at lower temperatures and shifts to chemisorption at higher temperatures. According to PP results, **H2NAET** works as mixed inhibitor. AFM approved the adsorption of **H2NAET** on the CS surface in 1 M HCl.

References

1 K.J. Al-Sallami, K. Shalabi, A.S. Fouda, (2021) Impact of Conyza bonariensis extract on the corrosion protection of carbon steel in 2 M HCl solution, *International Journal of Electrochemical Science*, 16 210929.

2 K. Chkirate, K. Azgaou, H. Elmsellem, B. El Ibrahimi, N.K. Sebbar, E.H. Anouar, M. Benmessaoud, S. El Hajjaji, E.M. Essassi, (2021) Corrosion inhibition potential of 2-[(5-methylpyrazol-3-yl)methyl]benzimidazole against carbon steel corrosion in 1 M HCl solution: Combining experimental and theoretical studies, *Journal of Molecular Liquids*, 321 114750.

3 H.M. Abd El-Lateef, A.R. Sayed, K. Shalabi, (2021) Synthesis and theoretical

studies of novel conjugated polyazomethines and their application as efficient inhibitors for C1018 steel pickling corrosion behavior, Surfaces and Interfaces, 23 101037.

4 Y. Boughoues, M. Benamira, L. Messaadia, N. Ribouh, (2020) Adsorption and corrosion inhibition performance of some environmental friendly organic inhibitors for mild steel in HCl solution via experimental and theoretical study, Colloids and Surfaces A: Physicochemical and Engineering Aspects, 593 124610.

5 G.E. Badr, (2009) The role of some thiosemicarbazide derivatives as corrosion inhibitors for C-steel in acidic media, Corrosion Science, **51** 2529-2536.

6 S. Shahabi, P. Norouzi, M.R. Ganjali, (2015) Electrochemical and theoretical study of the inhibition effect of two synthesized thiosemicarbazide derivatives on carbon steel corrosion in hydrochloric acid solution, RSC Advances, **5** 20838-20847.

7 S. Shahabi, P. Norouzi, (2017) Electrochemical and Quantum Chemical Assessment of Some Thiosemicarbazide Derivatives as Carbon Steel Corrosion Inhibitors in HCl; Continuously Monitoring the Current Change by FFT Voltammetry, *International Journal of Electrochemical Science,* **12** 2628-2646.

[8 A.M. Al-Bonayan, (2015) Inhibiting Effect of Thiosemicarbazide and 4-Phenyl Thiosemicarbazide Towards the Corrosion of Carbon Steel in H3PO4 Solutions, *International Journal of Electrochemical Science*, **10** 589-601.

9 P. Mohan, G.P. Kalaignan, 1, 4-Bis (2-nitrobenzylidene) (2013) thiosemicarbazide as Effective Corrosion Inhibitor for Mild Steel, *Journal of Materials Science & Technology*, **29** 1096-1100.

10 A.Y. Musa, A.A.H. Kadhum, A.B. Mohamad, M.S. Takriff, Molecular dynamics and quantum (2011) chemical calculation studies on 4,4-dimethyl-3-thiosemicarbazide as corrosion inhibitor in 2.5M H_2SO_4, Materials Chemistry and Physics, **129** 660-665.

11 O.A. El-Gammal, M.M. Bekheit, M. Tahoon, (2015) Synthesis, characterization and biological activity of 2-acetylpyridine-alpha naphthoxyacetylhydrazone and its metal complexes [corrected], Spectrochim Acta A Mol Biomol Spectrosc, **135** 597-607.

12 G. Sahin, E. Palaska, P. Kelicen, R. Demirdamar, G.J.A. Altinok, (2001) Synthesis of some new 1-acylthiosemicarbazides, 1,3,4-oxadiazoles, 1,3,4-thiadiazoles and 1,2,4-triazole-3-thiones and their anti-inflammatory activities, Arzneimittelforschung , 51 478-484.

13 A.S. Fouda, A. El-Askalany, A.T. El-Habab, S. Ahmed, (2019) Anticorrosion Properties of Some Nonionic Surfactants on Carbon Steel in 1 M HCl Environment, *Journal of Bio- and Tribo-Corrosion*, 5 56.

14 A.G. Sayed, A.M. Ashmawy, W.E. Elgammal, S.M. Hassan, M.A. Deyab, (2023) Synthesis, description, and application of novel corrosion inhibitors for CS AISI1095 in 1.0 M HCl based on benzoquinoline derivatives, Sci Rep, 13 13761.

15 A.H. El-Askalany, S.I. Mostafa, K. Shalabi, A.M. Eid, S. Shaaban, Novel tetrazole-based (2016) symmetrical diselenides as corrosion inhibitors for N80 carbon steel in 1 M HCl solutions: Experimental and theoretical studies, *Journal of Molecular Liquids*, **223** 497-508.

16 K. Shalabi, A.M. Helmy, A.H. El-Askalany, M.M. Shahba, (2019) New pyridinium bromide mono-cationic surfactant as corrosion inhibitor for carbon steel during chemical cleaning: Experimental and theoretical studies, *Journal of Molecular Liquids*, 293 111480.

17 A. Fouda, K. Shalabi, A. E-Hossiany, Moxifloxacin antibiotic as green corrosion inhibitor for carbon steel in (2016) 1 M HCl, *Journal of Bio- and Tribo-Corrosion*, 2 1-13.

18 H.M. Abd El-Lateef, K. Shalabi, A.A. Abdelhamid, (2021).One-pot synthesis of novel triphenyl hexyl imidazole

derivatives catalyzed by ionic liquid for acid corrosion inhibition of C1018 steel: Experimental and computational perspectives, *Journal of Molecular Liquids*, 334

19 M. Filali, E. El Hadrami, A. Bentama, B. Hafez, I. Abdel-Rahman, A. Harrach, H. Elmsellem, B. Hammouti, M. Mokhtari, S.E. Stiriba, and M. Julve, Inhibition, 3, 6-Di (pyridin-2-yl) (2019) pyridazine derivatives as original and new corrosion inhibitors in support of mild steel: Experimental studies and DFT investigational, *International Journal of Corrosion and Scale Inhibition*, **8** 93-109.

20 T.K. Sarkar, M. Yadav, I.B. Obot, (2022) Mechanistic evaluation of adsorption and corrosion inhibition capabilities of novel indoline compounds for oil well/tubing steel in 15% HCl, *Chemical Engineering Journal*, 431 133481.

21 A.S. Fouda, M.A. Ismail, R.M. Abou-shahba, W.A. Husien, E.S. El-Habab, A.S. Abousalem, (2020) Experimental and computational chemical studies on the cationic furanylnicotinamidines as novel corrosion inhibitors in aqueous solutions, Chinese *Journal of Chemical Engineering*, **28** 477-491.

22 K.M. Abd El-Khalek, K. Shalabi, M.A. Ismail, A.E.S. Fouda, 5-Arylidene-1,3-(2022) dialkylbarbituric acid derivatives as efficient corrosion inhibitors for carbon steel in molar hydrochloric acid solution, RSC Adv, **12** 10443-10459.

23 A.S. Fouda, F.I. El-Dossoki, A. El-Hossiany, E.A. Sello, (2020) Adsorption and Anticorrosion Behavior of Expired Meloxicam on Mild Steel in Hydrochloric Acid Solution, Surface Engineering and Applied Electrochemistry, 56 491-500.

24 A.S. Fouda, M.A. Ismail, A.A. Al-Khamri, A.S. Abousalem, (2019) Experimental, quantum chemical and molecular simulation studies on the action of arylthiophene derivatives as acid corrosion inhibitors, *Journal of Molecular Liquids*, 290 111178.